ALEXANDRIA ENGINEERING JOURNAL

Accepted March 4th 2017

ISSN: 1110-0168

PUBLISHER: ELSEVIER

NUMERICAL SOLUTION OF MHD SLIP FLOW OF A NANOFLUID PAST A RADIATING PLATE WITH NEWTONIAN HEATING: A LIE GROUP APPROACH

M.J. Uddin
Department of Mathematics, University Sains-Malaysia, ***Malaysia***
A. Sohail
Department of Mathematics, COMSATS- S Institute of Information Technology,Mathematica, Lahore, ***Pakistan***
O. Anwar Bég
Fluid Mechanics, Mechanical and Aeronautical Engineering, Newton Bldg, The Crescent, University of Salford, Manchester, M54WT, ***England, UK.***
M.J. Uddin
Department of Mathematics, University Sains-Malaysia, ***Malaysia***

ABSTRACT

In this paper, we have examined the magnetohydrodynamic flow of a nanofluid past a radiating sheet. The Navier velocity slip, Newtonian heating and passively controlled wall boundary conditions are considered. The governing equations are reduced into similarity equations with the help of Lie group. A collocation method is used for simulation. The influence of emerging parameters on velocity, temperature, nanoparticle volumetric fraction profiles, as well as on local skin friction factor and local Nusselt number are illustrated in detail. It is found that the friction (heat transfer rate) is lower (higher) for passively controlled boundary conditions as compared to the case of an actively controlled boundary condition. The magnetic field decreases both the skin friction and the rate of heat transfer. The findings are validated with existing results and found an excellent agreement. The model explores new applications in solar collectors with direct solar radiative input using magnetic nanofluids.

KEYWORDS: *Lie group, Navier slip flow; Newtonian heating, Nonlinear radiation, Passively controlled boundary condition, MHD.*

1.INTRODUCTION

Sustainable energy generation has emerged a critical issue in the global economic environment. The depletion of worldwide fossil fuels coupled with unacceptably high emissions has driven engineers and scientists to seriously consider new ecologically-friendly and sustainable energy systems. Solar energy is

one of the significant sources of renewable energy which can meet the future energy necessities. The sun, wind, biomass and hydropower constitute substantial sources of renewable energy. Scientists, engineers and applied mathematician are exploring these and other novel energy sources to develop new energy technologies which maintain clean and sustainable energy sources and to combat climate change. The most significant source of renewable energy is the sun. The energy found from nature in the form of solar radiation can be transformed into electricity without greenhouse emission. Investigators are paying attention to explore new technologies and sources for the sustainable energy [1]. Solar energy is one of the main sources of renewable energy with less environmental impact [2]. Solar power is widely used to produce electricity and heat from nature. Thermal radiative transport is also important in many engineering applications namely furnaces, forest fire dynamics, heating/cooling chambers, open water reservoirs and many other processes associated with the environment. Nanomaterials have emerged in the past decade or so as a new energy material. These materials are able to absorb thermal radiation. Solar collector designs have been proven to achieve enhanced performance using nanofluids. A review on the applications of nanofluids in solar energy systems is presented by Alibakhsh et al. [3]. It is mentioned that Hunt [4] was the first person who apply the idea of using small particles to collect solar energy.

It is now established both experimentally and theoretically that mixing nanoparticles in a liquid (a nanofluid) improves the thermophysical properties of the carrier fluid. Nanoparticles are capable of enhancing the radiative properties of liquids which interns improved the efficiency of the absorption of solar collectors. The heat transfer resulting from solar energy radiation is important due to its diverse engineering applications. The energy efficient heat transfer fluids are required to minimize the manufacturing and operating cost of hybrid-power engines, microelectronics, nano-electronics, fuel cells and pharmaceutical products. Effective coolants are required to keep the temperature of heat-generating devices within prescribed limits. Techniques that have been suggested to increase heat transfer in various situations can be classified into two major groups: (i) active techniques and (ii) passive techniques. In the case of *active* techniques, external energy is required namely, mechanical mixing, rotation, vibration, and magnetic field, which have been effectively applied to enhance heat/mass transfer, leading to efficient heat pumps,

separators and reactors and faster processing [5]. However external energy input is costly and inconvenient under compact situations [6]. P*assive* techniques, heat transfer amplification can be found by modifying fluids properties, surface geometry, surface roughness, special surface geometries, and suction/injection of fluid, fluid motion (laminar versus turbulent) or fluid additives (ultra-fine nano/micro-particles). However their inherent limitation is the relatively low thermal conductivity of heat transfer fluids [6]. Following Maxwell [7], many scholars investigated both theoretically and experimentally the influence of solid–liquid mixtures on augmentation of heat transfer. However this mixture encountered serious difficulties including abrasion, clogging, and fouling and extra pressure loss of the system, which becomes problematic for heat transfer systems [8]. To overcome these problems, Choi [9] introduced ultra-fine nanoparticles (<50 nanometers in diameter) dispersed in the base fluid and thereby introduced nanofluids. Nanofluids, a more efficient type of working fluid, are achieved by dissolving nanometer-sized particles/fibres between 1-100 nm with the conventional heat transfer fluids. Nanoparticles have *unique* mechanical, optical, electrical, magnetic, and thermal properties. The size of these suspended particles is of the order of a few nano-meters. Some commonly used nanoparticles are Al_2O_3, CuO, TiO_2, ZnO and SiO_2. The volume fraction of nanoparticles is normally engineered to be 3% to 5% [10], so that the nanofluid exhibits hydrodynamic behavior similar to the carrier fluid. Many models have been proposed to display the enhancement of thermal conductivity. It was shown by the previous researchers that, some of the factors responsible for enhance in thermal conductivity in nanofluids are (a) dispersion of nanoparticles [11], (b) the turbulence due to the presence of nanoparticles, and (c) the effect of the rotation of the nanoparticles [12]. A proper theory is required to estimate the thermal conductivity of a nanofluid. The theoretical models proposed by Maxwell-Garnett [13], Wang et al. [14] give much lower values than those acquired in the laboratory. Both experimental and theoretical results have revealed that for *forced* convective nanofluid flow, heat transfer characteristics are enhanced whereas the opposite trend is observed for *natural* convection. An experimental examination of natural convective heat transfer due to nanofluids was carried out by Putra et al. [15] and Wen and Ding [16]. They found that heat transfer rate *reduces* as concentration of nanoparticles enhances (contradicting Khanafer et al. [17]). Reviews have been conducted of the latest developments in nanofluid technology and are available in the papers of Wang and Mujumdar [18], Adnan et al. [19], Mahdi et al. [20],

Mauro et al. [21] etc. and in the monographs of Tiwari and Das [10], Sattler [22], Murshed et al. [23] and Minkowycz et al. [24] etc. Recently, many studies have been communicated deploying Buongiorno's model for both steady and unsteady nanofluid dynamics. Nield and Kuznetsov [25] studied the Cheng–Minkowycz problem of natural convective flow along a vertical plate. Kuznetsov and Nield [26] presented similarity solution of natural convective flow. The heat and mass transfer due to unsteady natural convective flow over a radiating vertical flat plate was studied by Turkyilmazoglu and Pop [27]. Recently, Kuznetsov and Nield [28] revised their previous model by incorporating passively controlled boundary condition to get physically realistic results. Sheikholeslami et al. [29] have reported the effect of thermal radiation on a magnetohydrodynamics nanofluid flow and heat transfer. The natural convective heat transfer flow past a horizontal plate was examined Zargartalebi et al. [30] taking into account variable thermophysical properties.

The magnetic field influences on flow, heat/mass transfer have received the attention of researcher due to many engineering applications. Examples include nuclear reactors, geothermal energy extraction, boundary layer control, electromagnetic launch technology etc. [31], manipulation of fluid flows in micro-devices, combustion control [32]. Magnetic nanofluids have many biomedical applications such as in intelligent biomaterials for wound treatment, gastric medications, sterilized devices etc. [33]. Some other significant applications relevant to industries are: crystal growth, MHD stirring of molten metal, and liquid metal cooling blankets for fusion reactors etc. [29]. Recent reviews addressing the applications of magnetic nanofluids can be found in Azizian et al. [34], Mehdi and Hangi [35], Kabeel et al. [36]. The magnetic field effects on convective nanofluid flow, heat and mass transfer past various geometries subject to various boundary conditions have been studied extensively. For example, natural convective flow past a stretching sheet was explored by Hamad [37]. Govindaraju et al. [38] computed the entropy generation in water based nanofluid flow. Ganesh et al. [39] studied the MHD flow of water based metal nanofluids. Rashidi et al. [40] considered the buoyancy effect on MHD flow of water based nanofluid. Kefayati [41] studied shear-thinning fluids in a lid-driven enclosure**.** Hakeem et al. [42] considered magnetic field effect on nanofluid over a

stretching/shrinking sheet. Some recent articles of nanofluids and their application are found in Dhanai et al. [43-45], Uddin et al. [46], Rana et al. [47-48].

Most of the mentioned researchers restricted their investigation to simple nanofluid boundary layer flows past a *vertical* surface. However, the natural convective heat transfer flow past a *horizontal* plate has received limited attention. Though**,** Pradhan *et al.* [49] explored the natural convective heat transfer flow past a stationary horizontal plate. They used convectional no-slip boundary conditions and constant nanoparticle volume fraction at the fluid-solid interface. However, no-slip boundary conditions and constant nanoparticle volume fraction at the wall can generate unrealistic results for heat and mass transfer rates [28, ,44]. In addition to the boundary conditions, sheet stretching is also an important characteristic in manufacture of nanomaterials. An experimental investigation carried by Vleggaar [51] revealed that the surrounding fluid motion can be idealized by a tangentially moving boundary with a velocity proportional to linear/nonlinear function of the distance from the slit. Hence to get physically realistic and practically applicable results, we have incorporated the simultaneous effects of velocity slip, Newtonian heating and zero mass flux boundary conditions on the boundary layer flow of nanofluid over an upward facing nonlinearly radiating horizontal stretching sheet. Solar radiation heat flux, as elaborated earlier, is of relevance to collector design and is therefore also analyzed in the present article.

2.NANOFLUID TRANSPORT MODEL

2.1 Assumptions

The two-dimensional steady viscous incompressible flow of a nanofluid over an upward facing non-linearly moving radiating horizontal plate is considered (Fig.1).

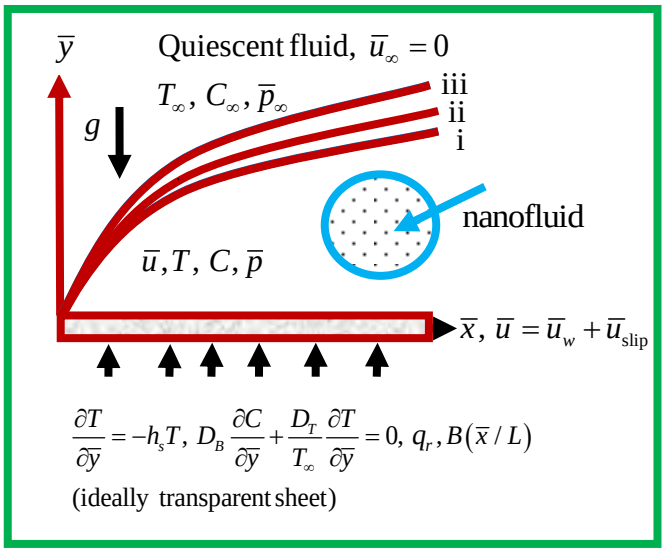

Fig. 1: Coordinate system and flow model.

The non-reflecting, non-absorbing, transparent semi-infinite sheet receives an incident radiation flux having intensity, q_r. This radiation flux penetrates the plate and absorbed in an adjacent fluid having absorption coefficient, k_1. Implicit in the Rosseland approximation employed to model uni-directional radiative flux is the high optical thickness of the fluid. The plate reduces heat to the ambient fluid having heat transfer coefficient h_s [62]. A variable magnetic field of strength, $B(\bar{x}/L) = B_0(\bar{x}/L)^{-4/5}$ (where B_0 is the constant magnetic field strength and L is the characteristic length), is applied perpendicular to the plate. One can expect that when $B(\bar{x}/L) = B_0(\bar{x}/L)^{-4/5}$, there is a singular point at $\bar{x} = 0$ (i.e. at the leading edge). However, the boundary layer equations are not true there. The induced magnetic field is assumed to be insignificant in comparison with the external magnetic field. Further, the imposed and induced electrical fields are assumed to be negligible. Newtonian heating boundary condition at the plate is imposed. It is assumed that the flow properties are constants except the density in the buoyancy terms. The field variables are: velocity vector $\vec{V}$, the temperature, T and the nanoparticle volume fraction) C.

2.2 Equations of the model

2.2.1 Dimensional form

Based on the above mentioned assumptions, the governing equations in dimensional form are below [28].

$$\nabla \cdot \vec{V} = 0, \qquad (1)$$

$$\rho\left[\frac{\partial \vec{V}}{\partial t}+\left(\vec{V}\cdot\nabla\right)\vec{V}\right]=-\nabla p+\nu\nabla^2\vec{V}+\left[C\rho_p+(1-C)\left\{\rho_f\left(1-\beta(T-T_\infty)\right)\right\}\right]\vec{g}+\vec{J}\times\vec{B}, \quad (2)$$

$$\left(\rho\, c_{\bar{p}}\right)_f\left(\frac{\partial T}{\partial t}+\vec{V}\cdot\nabla T\right)=k\nabla^2T+\left(\rho c_p\right)_p\left[D_B\nabla C\cdot\nabla T+\left(\frac{D_T}{T_\infty}\right)\nabla T\cdot\nabla T\right]-\frac{1}{\rho_f c_p}\frac{\partial q_r}{\partial \bar{y}}, \quad (3)$$

$$\frac{\partial C}{\partial t}+\vec{V}\cdot\nabla C=D_B\,\nabla^2C+\left(\frac{D_T}{T_\infty}\right)\nabla^2T. \quad (4)$$

Using Oberbeck–Boussinesq approximation, the momentum equation can be written as [28]:

$$\rho\left[\frac{\partial \vec{V}}{\partial t}+\left(\vec{V}\cdot\nabla\right)\vec{V}\right]=-\nabla \bar{p}+\nu\nabla^2\vec{V}+\left[\left(C-C_\infty\right)\left(\rho_{\bar{p}}-\rho_f\right)+\left(1-C_\infty\right)\rho_f\,\beta\left(T-T_\infty\right)\right]\vec{g}+\vec{J}\times\vec{B} \quad (5)$$

Here $\vec{J}=\sigma\vec{V}\times\vec{B}$ is the electrical current density and $\vec{B}$ is the magnetic induction vector. Using order of magnitude analysis so as, the governing equations are [43]:

$$\frac{\partial \bar{u}}{\partial \bar{x}}+\frac{\partial \bar{v}}{\partial \bar{y}}=0, \quad (6)$$

$$\rho_f\left(\bar{u}\frac{\partial \bar{u}}{\partial \bar{x}}+\bar{v}\frac{\partial \bar{u}}{\partial \bar{y}}\right)=-\frac{\partial \bar{p}}{\partial \bar{x}}+\mu\frac{\partial^2\bar{u}}{\partial \bar{y}^2}-\frac{\sigma B_0^2}{x^{2/5}}\bar{u}, \quad (7)$$

$$-\frac{\partial \bar{p}}{\partial \bar{y}}+\left[\left(1-C_\infty\right)\rho_f\, g\,\beta\left(T-T_\infty\right)-\left(\rho_{\bar{p}}-\rho_f\right)g\left(C-C_\infty\right)\right]=0, \quad (8)$$

$$\bar{u}\frac{\partial T}{\partial \bar{x}}+\bar{v}\frac{\partial T}{\partial \bar{y}}=\alpha\frac{\partial^2T}{\partial \bar{y}^2}+\tau\left[D_B\frac{\partial C}{\partial \bar{y}}\frac{\partial T}{\partial \bar{y}}+\left(\frac{D_T}{T_\infty}\right)\left(\frac{\partial T}{\partial \bar{y}}\right)^2\right]-\frac{1}{\rho_f c_p}\frac{\partial q_r}{\partial \bar{y}}, \quad (9)$$

$$\bar{u}\frac{\partial C}{\partial \bar{x}}+\bar{v}\frac{\partial C}{\partial \bar{y}}=D_B\frac{\partial^2C}{\partial \bar{y}^2}+\left(\frac{D_T}{T_\infty}\right)\frac{\partial^2T}{\partial \bar{y}^2}. \quad (10)$$

The relevant boundary conditions are [44],

$$\bar{u}=\lambda\,\bar{u}_w\left(\bar{x}/L\right)+\bar{u}_{\text{slip}},\bar{v}=0,\ k\frac{\partial T}{\partial \bar{y}}=-h_s\left(\bar{x}/L\right)T\ (\text{NH}),\ T=T_w\ (\text{IP}),$$

$$D_B\frac{\partial C}{\partial \bar{y}}+\frac{D_T}{T_\infty}\frac{\partial T}{\partial \bar{y}}=0 \text{ at } \bar{y}=0, \quad (11)$$

$$\bar{u}\to 0,\ T\to T_\infty,\ C\to C_\infty,\ \bar{p}\to \bar{p}_\infty \text{ as } \bar{y}\to\infty,$$

where $\alpha = \dfrac{k}{\left(\rho\, c_{\bar{p}}\right)_f}$ is the thermal diffusivity of the fluid and $\tau = \dfrac{\left(\rho\, c_{\bar{p}}\right)_{\bar{p}}}{\left(\rho\, c_{\bar{p}}\right)_f}$ is the ratio of heat capacities, ρ_f is the density of the base fluid, μ is the dynamic viscosity of the base fluid, β is the volumetric expansion coefficient of nanofluid, $\rho_{\bar{p}}$ is the density of the nanoparticles, $\left(\rho c_{\bar{p}}\right)_f$ is the heat effective heat capacity of the fluid, $\left(\rho\, c_{\bar{p}}\right)_{\bar{p}}$ is the effective heat capacity of the nanoparticle material, k is the effective thermal conductivity, $\vec{g}$ is the gravitational acceleration. Here D_B represents the Brownian diffusion coefficient and D_T signifies for the thermophoretic diffusion coefficient, $\bar{u}_w\left(\bar{x}/L\right) = \lambda \dfrac{\alpha}{L} Ra^{2/5} \left(\dfrac{\bar{x}}{L}\right)^{1/5}$ is the velocity of the sheet, $\bar{u}_{\text{slip}} = \dfrac{\mu}{\rho} N_1\left(\bar{x}/L\right) \dfrac{\partial \bar{u}}{\partial \bar{y}}$ is the variable linear slip velocity, $N_1\left(\dfrac{\bar{x}}{L}\right) = \left(N_1\right)_0 \left(\dfrac{\bar{x}}{L}\right)^{2/5}$ is the velocity slip factor with $\left(N_1\right)_0$ constant velocity slip factor, $h_s\left(\dfrac{\bar{x}}{L}\right) = \left(h_s\right)_0 \left(\dfrac{\bar{x}}{L}\right)^{2/5}$ is the variable heat transfer coefficient, $\left(h_s\right)_0$ is the constant heat transfer coefficient, $\lambda > 0$ is associated with a stretching sheet, $\lambda < 0$ corresponds to a shrinking sheet and $\lambda = 0$ stands for stationary plate. We assumed that the boundary layer is optically thick and the Rosseland diffusion approximation for radiation is valid [53]. Thus, the radiative heat flux for an optically thick boundary layer (with intensive absorption) is defined as $q_r = -\dfrac{4\sigma_1}{3k_1} \dfrac{\partial T^4}{\partial \bar{y}}$, where σ_1 (=5.67×10−8 W/m^2 K^4) is the Stefan-Boltzmann constant and k_1 (m^{-1}) is the Rosseland mean absorption coefficient [54].

2.2.2 Non-dimensional form

Following non-dimensional variables are introduced to normalize Eqns. (6)-(11):

$$
\begin{aligned}
&x = \frac{\bar{x}}{L},\quad y = \frac{\bar{y}}{L} Ra_L^{1/5},\quad u = \frac{L}{\alpha} Ra_L^{-2/5} \bar{u},\quad v = \frac{L}{\alpha} Ra_L^{-1/5}\, \bar{v},\quad \theta = \frac{T - T_\infty}{T_\infty}\,(\text{NH}),\\
&\theta = \frac{T - T_\infty}{T_w - T_\infty}\,(\text{IP}),\quad \phi = \frac{C - C_\infty}{C_\infty},\quad p = \frac{L^2\left(\bar{p} - \bar{p}_\infty\right)}{\rho_f \alpha^2} Ra_L^{-4/5},
\end{aligned}
\tag{12}
$$

where $Ra_L = g\beta(1-C_\infty)T_\infty L^3\rho_f/(\alpha\mu)$ is the Rayleigh number based on characteristic length L. A dimensionless stream function ψ defined by

$$u = \frac{\partial\psi}{\partial y} \text{ and } v = -\frac{\partial\psi}{\partial x}, \tag{13}$$

is introduced into Eqns. (7)-(10), leading to

$$\mathrm{Pr}\frac{\partial^3\psi}{\partial y^3} - \frac{\partial p}{\partial x} + \frac{\partial\psi}{\partial x}\frac{\partial^2\psi}{\partial y^2} - \frac{\partial\psi}{\partial y}\frac{\partial^2\psi}{\partial y\partial x} + M\frac{1}{x^{2/5}}\frac{\partial\psi}{\partial y} = 0, \tag{14}$$

$$-\frac{1}{\mathrm{Pr}}\frac{\partial p}{\partial y} + \theta - Nr\phi = 0, \tag{15}$$

$$\frac{\partial\psi}{\partial y}\frac{\partial\theta}{\partial x} - \frac{\partial\psi}{\partial x}\frac{\partial\theta}{\partial y} - \frac{\partial^2\theta}{\partial y^2} - Nb\frac{\partial\theta}{\partial y}\frac{\partial\phi}{\partial y} - Nt\left(\frac{\partial\theta}{\partial y}\right)^2 - \frac{4}{3R}\frac{\partial}{\partial y}\left[\{1+(T_r-1)\theta\}^3\frac{\partial\theta}{\partial y}\right] = 0, \tag{16}$$

$$Le\left[\frac{\partial\psi}{\partial y}\frac{\partial\phi}{\partial x} - \frac{\partial\psi}{\partial x}\frac{\partial\phi}{\partial y}\right] - \frac{\partial^2\phi}{\partial y^2} - \frac{Nt}{Nb}\frac{\partial^2\theta}{\partial y^2} = 0. \tag{17}$$

The boundary conditions in Eqn. (11) become

$$\begin{aligned} &\frac{\partial\psi}{\partial x} = 0, \frac{\partial\psi}{\partial y} = \lambda a\, x^{1/5}\frac{\partial^2\psi}{\partial y^2}, \frac{\partial\theta}{\partial y} = -\gamma\, x^{-2/5}(1+\theta)\,(\mathrm{NH}), \theta = 1(\mathrm{IP}), Nb\,\phi' + Nt\,\theta' = 0 \text{ at } y = 0, \\ &\frac{\partial\psi}{\partial y} \to 0, \quad \theta \to 0, \quad \phi \to 0, \; p \to 0 \text{ as } y \to \infty. \end{aligned} \tag{18}$$

Ten dimensionless parameters feature in Eqns. (14)-(18) and are defined as: $\mathrm{Pr} = \frac{\nu}{\alpha}$ (Prandtl number), $Nt = \frac{\tau D_T}{\alpha}$ (thermophoresis), $Nb = \frac{\tau D_B C_\infty}{\alpha}$ (Brownian motion), $Nr = \frac{(\rho_p - \rho_f)C_\infty}{\rho_f\beta(1-C_\infty)T_\infty}$ (buoyancy ratio), $Le = \frac{\alpha}{D_B}$ (Lewis number), $a = \frac{(N_1)_0\,\mu Ra_L^{2/5}}{\rho_f L}$ (velocity slip), $\gamma = \frac{(h_s)_0 L}{k\,Ra^{2/5}}$ (Newtonian heating), $M = \frac{\sigma B_0^2 L^2}{\alpha Ra_L^{2/5}}$ (magnetic field), $T_r = \frac{T_w}{T_\infty}$ (wall temperature excess ratio), $R = \frac{k\,k_1}{4\sigma_1 T_\infty^3}$ (convection-radiation).

3.SYMMETRY GROUP OF THE PROBLEM

The similarity solution plays an important role in many fields in sciences and engineering. The Lie group transformation technique is a well-developed theory on continuous symmetry of mathematical objects and structures. It can be used in many areas of applied mathematics, theoretical physics and engineering problems. This theory can provide methodology for analyzing the continuous symmetries of the governing equations. The application of this technique reduces the number of independent variables of the governing partial differential equations under consideration and remains the system and relevant initial and boundary conditions *invariant*. Many researchers used the Lie group transformation technique to various transport problems. Examples include Ma et al. [55], Kolomenskiy and Mofatt [56], Asghar et al. [57], and Uddin et al. [58]. Reviews for the theory and applications of Lie group analysis to differential equations can be found in the texts by Seshadri and Na [59], Olver [60], Cantwell [61], Bluman and Anco [62]. Using Lie group method to Eqns. (14)-(17), the infinitesimal generator for the problem can be written as

$$X = \xi_1 \frac{\partial}{\partial x} + \xi_2 \frac{\partial}{\partial y} + \eta_1 \frac{\partial}{\partial \psi} + \eta_2 \frac{\partial}{\partial \theta} + \eta_3 \frac{\partial}{\partial \phi} + \eta_4 \frac{\partial}{\partial p}, \tag{19}$$

where the transformations are $(x, y, \psi, \theta, \phi, p)$ to $(x^*, y^*, \psi^*, \theta^*, \phi^*, p^*)$. The infinitesimals $\xi_1, \xi_2, \eta_1, \eta_2, \eta_3$ and η_4 satisfy the following equations

$$\begin{aligned}
&\frac{dx^*}{d\varepsilon} = \xi_1(x^*, y^*, \psi^*, \theta^*, \phi^*, p^*), \ \frac{dy^*}{d\varepsilon} = \xi_2(x^*, y^*, \psi^*, \theta^*, \phi^*, p^*), \\
&\frac{d\psi^*}{d\varepsilon} = \eta_1(x^*, y^*, \psi^*, \theta^*, \phi^*, p^*), \ \frac{d\theta^*}{d\varepsilon} = \eta_2(x^*, y^*, \psi^*, \theta^*, \phi^*, p^*), \\
&\frac{d\phi^*}{d\varepsilon} = \eta_3(x^*, y^*, \psi^*, \theta^*, \phi^*, p^*), \ \frac{dp^*}{d\varepsilon} = \eta_4(x^*, y^*, \psi^*, \theta^*, \phi^*, p^*).
\end{aligned} \tag{20}$$

After tedious algebraic manipulation, the infinitesimals are

$$\begin{aligned}
&\xi_1 = c_1 x + c_2, \quad \xi_2 = \frac{2}{5} c_1 y + c_3, \\
&\eta_1 = \frac{3}{5} c_1 \psi + c_4, \ \eta_2 = c_5, \ \eta_3 = c_6, \eta_4 = (c_5 + c_6) y + \frac{2}{5} c_1 p,
\end{aligned} \tag{21}$$

where $c_i \, (i = 1, 2, \cdots, 6)$ are arbitrary constants. Hence, the equations admit *six finite parameter Lie group* transformations. Note that the parameters c_2, c_3 correspond to the translation in the variables x, y, the parameters c_5, c_6 correspond to the translation in the variables θ, ϕ and the parameter c_4 corresponds to the

translation in the variable ψ. The parameter c_1 corresponds to the scaling in the variables x, y, ψ and p respectively. The characteristic equation is

$$\frac{dx}{c_1 x + c_2} = \frac{dy}{\frac{2}{5}c_1 y + c_3} = \frac{d\psi}{\frac{3}{5}c_1\psi + c_4} = \frac{d\theta}{c_5} = \frac{d\phi}{c_6} = \frac{dp}{-\alpha_2\left(c_5 + c_6\right)y + \frac{2}{5}c_1 p}. \quad (22)$$

From Eqn. (22), the invariants are:

$$\eta = \frac{y}{x^{\frac{2}{5}}},\ \psi = x^{\frac{3}{5}} f(\eta),\ p = x^{\frac{2}{5}} h(\eta),\ \theta = \theta(\eta),\ \phi = \phi(\eta). \quad (23)$$

For simplicity we assume that $c_i = 0, (i = 2-6)$. Here $f(\eta), \theta(\eta)$ and $\phi(\eta)$ represent the no-dimensional velocity, temperature and concentration.

3.2 Similarity Equations

Substituting (23) into Eqns. (14) - (18), we obtain:

$$\mathrm{Pr}\, f''' + \frac{3}{5} f\, f'' - \frac{1}{5} f'^2 + \frac{2}{5}\eta h' - \frac{2}{5} h - M\, f' = 0, \quad (24)$$

$$-\frac{1}{\mathrm{Pr}} h' + \theta - Nr\, \phi = 0, \quad (25)$$

$$\theta'' + \frac{3}{5} f\, \theta' + Nb\, \theta'\, \phi' + Nt\, \theta'^2 + \frac{4}{3R}\left[\left\{1 + \left(T_r - 1\right)\theta\right\}^3 \theta'\right]' = 0, \quad (26)$$

$$\phi'' + \frac{3}{5} Le\, f\, \phi' + \frac{Nt}{Nb}\theta'' = 0. \quad (27)$$

The relevant boundary conditions in Eqn. (19) transformed to

$$\begin{aligned} &f = 0,\ f' = \lambda + a\, f'',\ \theta' = -\gamma\left[1 + \theta\right]\text{(NH)},\ \theta = 1\text{(IP)},\ Nb\,\phi' + Nt\,\theta' = 0 \text{ at } \eta = 0, \\ &f' = h = \theta = \phi = 0 \text{ as } \eta \to \infty, \end{aligned} \quad (28)$$

where primes represent ordinary differentiation with respect to η.

4. FRICTION AND HEAT TRANSFER RATES

The knowledge of drag and heat transfer rates at the wall is essential in order to evaluate the performance of the various microfluidic/nanofluidics and thermal devices. The information related to wall property variation

provides information which enables improvement in the design of devices for superior performance and efficiency [63]. Thus the skin friction and heat transfer are key quantities that should be quantified. These quantities can be calculated from the following relations:

$$C_{f\bar{x}} = \frac{2\mu}{\rho U_r^2}\left(\frac{\partial \bar{u}}{\partial \bar{y}}\right)_{\bar{y}=0}, \quad Nu_{\bar{x}} = \frac{-\bar{x}}{T_w - T_\infty}\left(\frac{\partial T}{\partial \bar{y}}\right)_{\bar{y}=0}. \tag{29}$$

Here $U_r = g\beta(1-C_\infty)T_\infty L^2/\alpha$ is the characteristic velocity.

By substituting from Eqns. (12) and (23) into Eqn. (29), we get

$$Ra_{\bar{x}}^{7/5}\,\mathrm{Pr}\,C_{f\bar{x}} = f''(0),\; Ra_{\bar{x}}^{-1/5}\,Nu_{\bar{x}} = -\left[1+\frac{4}{3R}\left\{1+(T_r-1)\theta(0)\right\}^3\right]\frac{\theta'(0)}{\theta(0)}. \tag{30}$$

Here $Ra_{\bar{x}} = g\beta(1-C_\infty)T_\infty \bar{x}^3/(\alpha\nu)$ is the local Rayleigh number.

5. VALIDATION OF MODEL

It is worth mentioning that in the case of hydrodynamic boundary layer flow past a non-radiating ($R\to\infty$), isothermal ($\theta(0)=1$) stationary plate with no slip boundary conditions at wall ($M=a=\lambda=0$) the problem under consideration reduces to the problem investigated by Pradhan et al. [49] which validates our symmetry group analysis.

6. NUMERICAL SOLUTION

The governing equations are transformed to ordinary differential equations with the help of Lie symmetry group method. We will solve the equations (23)-(27) subject to boundary conditions in Eqn. (28) numerically using a collocation method. The main advantage of this method is that, it reduces the n^{th} order differential equation (s) into *n* first order differential equations, thus reducing the computational cost on a large domain with small step size and a range of parameters. We have simplified the system of equations (24)-(28) using the Collocation Method (CM). For the validation of our numerical solution, we have solved the system of Eqns. (24)-(27) subject to the actively controlled boundary condition for which $\phi(0)=1$. We

have also presented the comparison in **Table 1**. An examination of this table reveals that our results are in agreement with the results of Pradhan et al. [49] which validates the accuracy of the present numerical code.

Table 1: Values of $f''(0)$ and $-\theta'(0)$ for *Nr=Nt=Nb=0.5, Pr =6.8.*

Le	$f''(0)$		$-\theta'(0)$	
	[49]	Present work	[49]	Present work
5	0.8435	0.8435	0.3268	0.3265
10	0.8806	0.8806	0.3239	0.3238
100	0.9217	0.9218	0.3135	0.3134

7. RESULTS AND DISCUSSION

7.1 Variations of the dimensionless velocity with M, R, γ and *Le*

Figures 2a-2b show the effects of the magnetic field (*M*), radiation parameter (*R*), Lewis number (*Le*), and Newtonian heating parameter (γ) on the non-dimensional velocity. It is observed that increasing *M* depresses the velocity field and the corresponding boundary layer thickness (Fig. 2a). Magnetic field therefore controls momentum diffusion rates and serves as a strong decelerating mechanism. It is also found from the same figure (Fig. 2a) that increasing the strength of the radiation parameter also depresses the flow velocity for both magnetohydrodynamic flow and purely hydrodynamic *(M=0)* flow. It is observed that increasing γ boosts the velocity field as well as velocity boundary layer thickness (Fig. 2b). It is further found from the same figure (Fig.2b) that increasing the Le also boosts the flow velocity. From, definition of Lewis number, it is clear that an increase of Le represent a higher thermal diffusivity of the fluid (α) for a constant mass diffusivity (D_B). This increases the flow within the boundary layer. For *Le<1* the species diffusivity exceeds thermal diffusivity and vice versa for *Le>1*. For *Le*=1 both thermal and species diffusivity will be of same order.

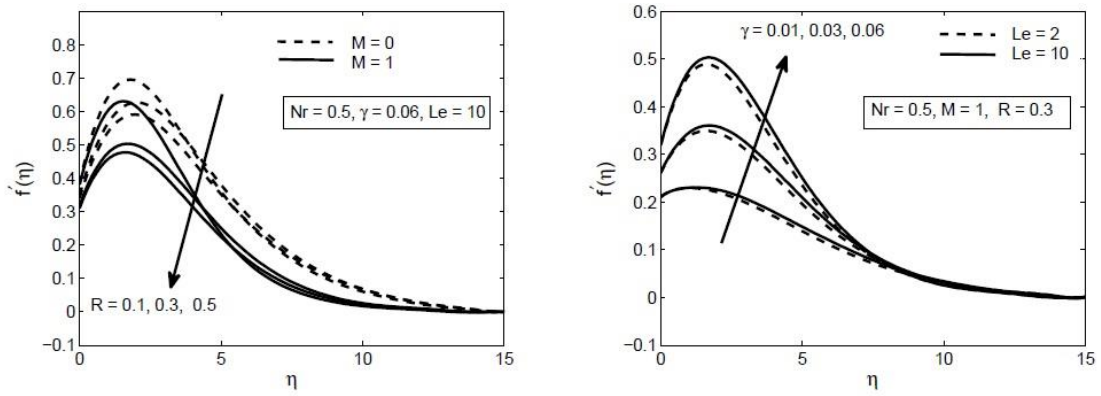

Figure 2: Effect of M, R, γ and Le on the velocity.

7.2 Variations of the dimensionless temperature with M, R, γ

The effects of the magnetic field (*M*), radiation parameter (*R*) and Newtonian heating parameter (γ) on the non-dimensional temperature are displayed in Figs. 3a and 3b. It is found that increasing *M increases* the temperature and corresponding thickness of the thermal boundary layer. Temperature is minimum for non-magnetic flow. Physically this is due to supplementary work is used in dragging the fluid against the action of the magnetic field and this is expended as thermal energy, heating the boundary layer. Thermal boundary layer thickness is therefore enhanced with increasing strength of magnetic field. The aiding effect of the magneto-hydrodynamics body force on the thermal diffusion also helps to elevate the nanoparticle volume fraction values . Stronger magnetic field therefore controls the flow field but enhances thermal and species diffusion. It is evident from Figs. 3 and 4 that temperature is much greater than nanoparticle volume fraction. It should be noted that the present simulations are valid for small magnetic Reynolds numbers (which relates the ratio of the fluid flux to the magnetic diffusivity) which is not adequately large for the magnetic field so as to be distorted by the flow. In the case of large magnetic Reynolds number, magnetic induction effects must be considered and will be communicated in the future. As with the velocity distribution, Newtonian heating parameter γ also boosts the temperature and thermal boundary layer thickness. The influences of *M* and *R* on the non-dimensional temperature are shown in Fig.3b. The temperature is decreased as the nonlinear radiation parameter *R* increases (Fig. 3b). Note that the parameter, *R*, signifies the contribution of thermal conduction heat transfer to the thermal radiation heat transfer $\left(R = \frac{k\, k_1}{4\sigma_1 T_\infty^3} \right)$. It appears in the energy conservation Eqn. (21) as a denominator. Therefore for higher

R values, the reduced contribution from the radiative mode of heat transfer will be exhibited by a decrease in temperature. A similar trend of temperature is reported by Pantokratoras and Fang [64]. It is found that temperature is increased as the Newtonian heating parameter is increased. Physically Newtonian heating implies that the heat transfer from the plate surface is *proportional* to the local surface temperature, as simulated in the wall thermal boundary condition in Eq. (22). The effect is prominent for even low values of γ. Temperature is clearly maximized with high γ. This thermal boundary condition therefore is of significant use in both peak solar heating situations and magnetic materials processing, in which higher temperatures are experienced at the wall. A similar conclusion is also drawn by Imtiaz et al. [65].

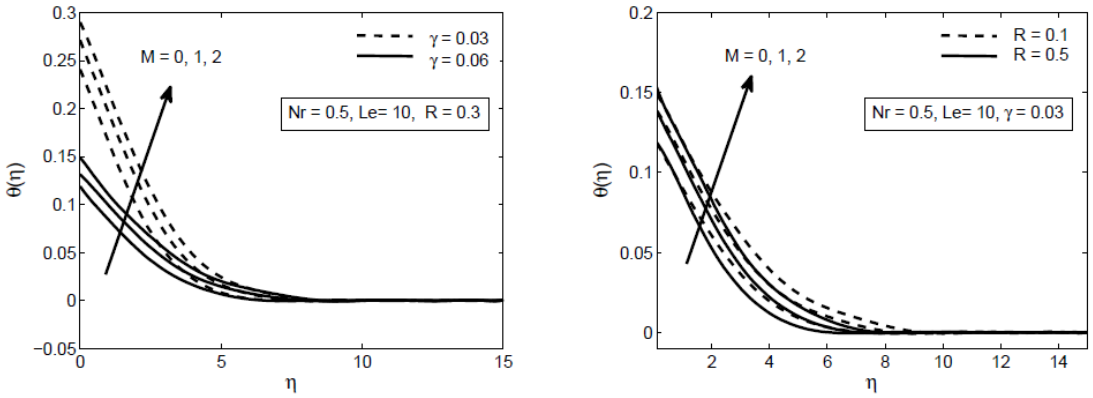

Figure 3: Effect of M, R, γ and Le on the temperature.

7.3 Variations of the dimensionless nanoparticle volume fraction with M, R, γ

Figures 4a-4b are drawn to display the effects of the magnetic field (*M*), radiation parameter (*R*), and Newtonian heating parameter (γ) on the dimensionless concentration. From Fig.4a it is revealed that increasing magnetic field parameter (*M*) enhances the concentration field as well as concentration boundary layer thickness. It is found from the same figure (Fig.4a) that increasing the strength of the Newtonian heating parameter depresses the concentration for both magnetohydrodynamic flow and purely hydrodynamic *(M=0)* flow. From Fig.4b it is evident that increasing radiation parameter *R* boosts the concentration as well as concentration boundary layer thickness. Decreasing thermal radiation flux therefore exacerbates nano-particle diffusion and the radiation effect needs to be addressed carefully to achieve a compromise in nano-particle distribution in the medium, since the latter aids thermal diffusion.

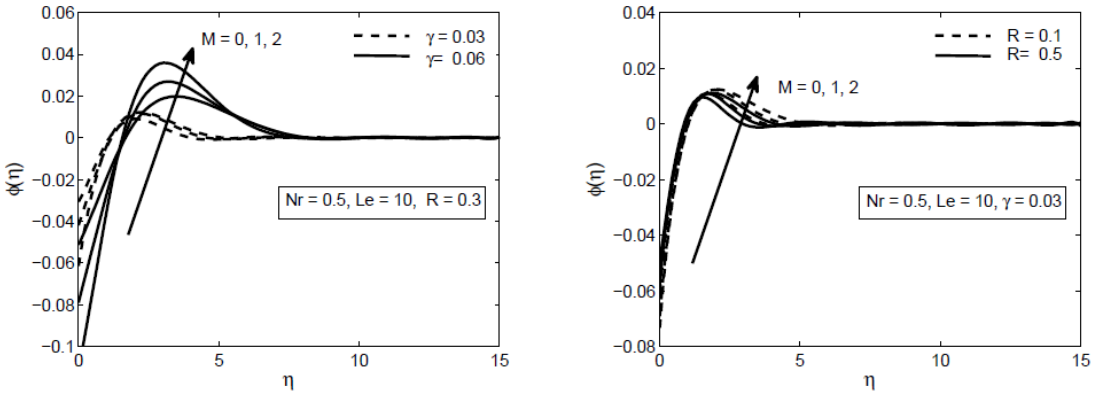

Figure 4: Effect of M, R, γ on the nanoparticle volume fraction.

7.4 Variation of the dimensionless friction factor with M, R, γ

We now focus our attention to thermal engineering design quantities. Figures 5-6 depict the effect of the various parameters on the dimensionless friction, and the heat transfer rates. The friction is decreased as the magnetic field parameter increases (Fig.5a) for both actively and passively controlled boundary conditions. The friction factor for passively controlled boundary condition is lower than that achieved with an actively controlled boundary condition (Fig. 5a-5b). Hence to reduce friction, a passively controlled boundary condition appears more promising. Friction is increased with the conduction-radiation and Newtonian heating parameters.

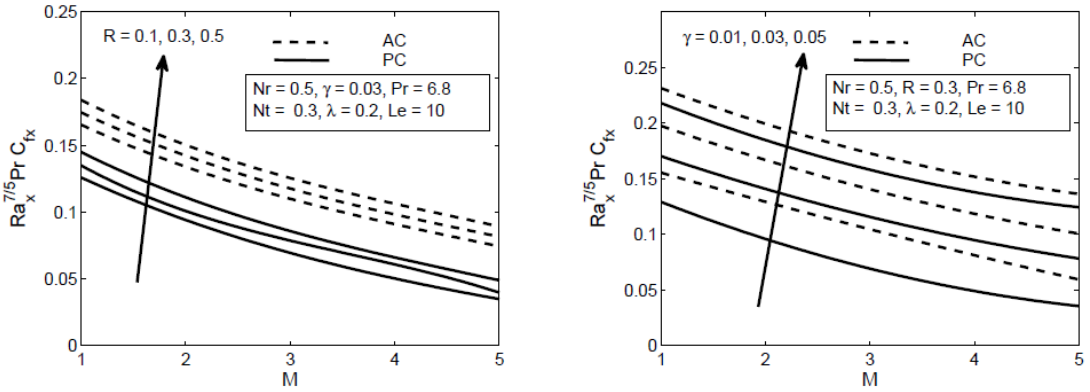

(a) (b)

Figure 5 : Effect of M, R, γ on the nanoparticle friction.

7.5 Variation of the dimensionless heat transfer rate with M, R, γ

It is observed from Fig.6 that heat transfer rates decreases with the magnetic field, and conduction-radiation parameter and increases with the Newtonian heating parameter for both actively and passively controlled boundary conditions. Note heat transfer rate is higher for passively controlled boundary conditions compared to actively controlled boundary condition.

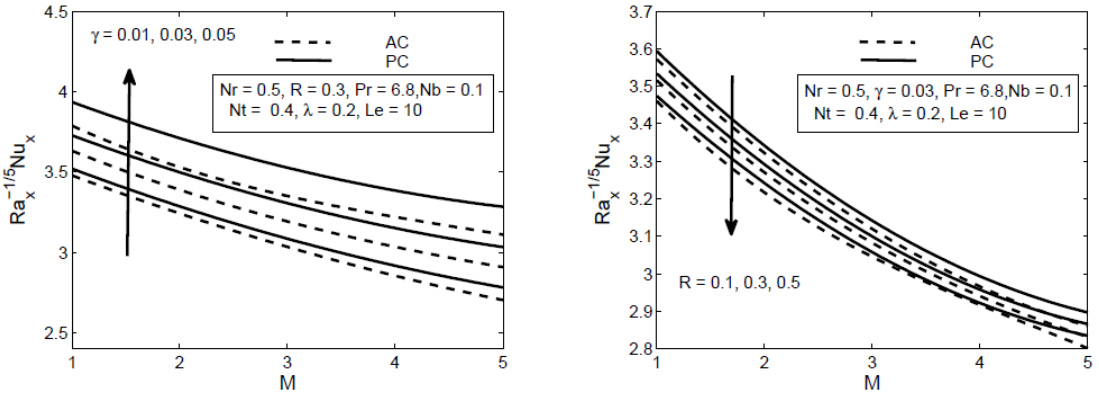

(a) (b)

Figure 6 : Effect of M, R, γ on the heat transfer rates.

7.6 Variation of the dimensionless heat transfer rate and skin friction with M, T_r .

Figures 7 a and b shows the effects of *M* and *Tr* on the dimensionless heat transfer rates and friction.

From figure 7 *a* it is noticed that heat transfer rates increases as wall excess temperature ratio increases for both actively controlled and passively controlled boundary condition. It is observed from figure 7b that heat friction increases with the wall excess temperature ratio for both actively and passively controlled boundary conditions.

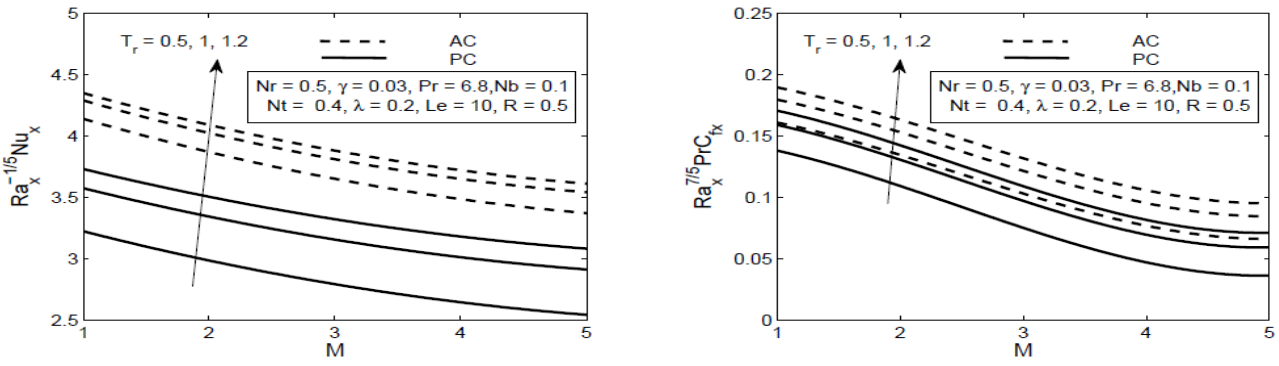

(a) (b)

Figure 7 : Effect of M, T_r on the heat transfer rates and skin friction .

8. CONCLUSIONS

Steady-state nanofluid flow from an upward facing radiating horizontal sheet has been illustrated by combined Lie symmetry group and numerical analysis techniques. Navier velocity slip, Newtonian heating effects and zero mass flux boundary conditions have been used to get realistic results. With the aid of Lie symmetry group method, the transport equations have been reduced to a nonlinear, coupled system of similarity equations. The resulting equations have been solved numerically using a Generalized Collocation Method. Solutions have been verified with previous results from the literature and very good correlation is obtained. The present computations have shown that:

(i) Friction is decreased as the velocity slip and sheet stretching parameters increase

(ii) Friction factor for passively controlled boundary condition is lower than that of actively controlled boundary condition.

(iii) Heat transfer rate decreases with the thermal slip, conduction-radiation but increases with Newtonian heating parameter

(iv) Heat transfer rate is higher for passively controlled boundary conditions compare to actively controlled boundary condition.

The finding of the present paper can be used to enhance the performances of the solar collectors as well as by the experimentalists in designing various thermal devices. The present study can be extended for unsteady flow and various non-Newtonian fluids, and efforts in this direction will be communicated in the near future.

ACKNOWLEDGEMENTS

The authors would like to acknowledge financial support from Universiti Sains Malaysia RU grant 1001/PMATHS/811252.

REFERENCES

[1] R. Kandasamy, I. Muhaimin, A.K. Rosmila, The performance evaluation of unsteady MHD non-Darcy nanofluid flow over a porous wedge due to renewable (solar) energy, Renew. Ener., 64,1-9(2014).

[2] A.K. Angstrom, Solar and atmospheric radiation, J Roy Meteorol Soc., 50, 121-6(1924).

[3] K. Alibakhsh, A.T. Eshghi, M. Sameti, A review on the applications of nanofluids in solar energy systems, Renew. and Sus. Ener. Rev. 43, 584-598, (2015)

[4] A.J. Hunt, Small particle heat exchangers, J Renew Sustain Energy Lawrence Berkeley Lab Report Number LBL-7841, 1978.

[5] A.E. Bergles, Heat transfer augmentation, in: *S. Kakaç, A. Bergles,E. O. Fernandes(Eds.), Two-Phase Flow Heat Exchangers*, Springer, Netherlands, 343–373, (1988).

[6] D. Wen, G. Lin, S. Vafaei, K. Zhang, Review of nanofluids for heat transfer applications, Particuology, 7, 141–150, (2009).

[7] J.C. Maxwell, *A Treatise on Electricity and Magnetism* (2nd ed.), Clarendon Press, Oxford, Uk (1873).

[8] M.J. Uddin, W.A. Khan, A.I.MD. Ismail, Free convection boundary layer flow from a heated upward facing horizontal flat plate embedded in a porous medium filled by a nanofluid with convective boundary condition, *Trans. in Porous Med.*, 92, 867-881, (2012).

[9] S.U.U Choi, Enhancing thermal conductivity of fluids with nanoparticle. In: *Development and applications of non-Newtonian flow, FED-vol. 231/MD-vol 66. ASME* 99–105, *(*1995).

[10] Das, S.K., Choi, S.U.S., Yu, W., and Pradeep, T., Nanofluids: Science and Technology, 1st ed., Wiley, New York, 2007.

[11] J. Buongiorno, Convective transport in nanofluids, ASME J. Heat Transfer, 128, 240–250, (2006).

[12] Y. Xuan, Q. Li, Investigation on convective heat transfer and flow features of nanofluids, ASME J. Heat Transfer, 125, 151–155, (2003).

[13] J.C. Maxwell-Garnett, Colours in metal glasses and in metallic films, Philos. Trans. R. Soc. London, Ser. A, 203, 385–420, (1904).

[14] B.X. Wang, L.P. Zhou, X.F. Peng, A fractal model for predicting the effective thermal conductivity of liquid with suspension of nanoparticles, Int. J. Heat Mass Transfer, 46, 2665–2672, (2003).

[15] N. Putra, W. Roetzel, S.K. Das, Natural convection of nano-fluids, Heat Mass Transfer, 39,775–784, (2003).

[16] D. Wen, Y. Ding, Natural convective heat transfer of suspensions of titanium dioxide nanoparticles (nanofluids), IEEE Trans. Nanotechnol., 5, 220–227, (2006).

[17] K. Khanafer, K. Vafai, M. Lightstone, Buoyancy-driven heat transfer enhancement in a two-dimensional enclosure utilizing nanofluidsInt. J. Heat Mass Transfer, 46,3639–3653, (2003).

[18] X.Q. Wang, A.S. Mujumdar, Heat transfer characteristics of nanofluids: a review, Int. J. Therm. Sci., 46, 1–19, (2007).

[19] H. Adnan, K.V. Sharma, R.A. Bakar, K. Kadirgama, A review of forced convection heat transfer enhancement and hydrodynamic characteristics of a nanofluid, *Renew. and Sus. Ener. Rev.,* 29, 734-743, (2014).

[20] R.A. Mahdi, H. A. Mohammed, K. M. Munisamy, N.H. Saeid, Review of convection heat transfer and fluid flow in porous media with nanofluid, *Renew. and Sus. Ener. Rev.,* 41, 715-734, (2015).

[21] L. Mauro, G. Colangelo, M. Milanese, A. de Risi, Review of heat transfer in nanofluids: Conductive, convective and radiative experimental results, *Renew. and Sus. Ener. Rev.*, 43,1182-1198, (2015).

[22] K.D. Sattler, Handbook of Nanophysics: Nanomedicine and Nanorobotics. CRC Press, New York, (2010).

[23] S.M.S. Murshed, K.C. Leong, C. Yang, Thermophysical properties of nanofluids. CRC Press, New York, (2011).

[24] W.J Minkowycz, E.M Sparrow, J.P Abraham, Nanoparticle Heat Transfer and Fluid Flow, CRC Press, Boca Raton, FL, New York, (2012).

[25] D.A. Nield, A.V. Kuznetsov, The Cheng-Minkowycz problem for natural convective boundary-layer flow in a porous medium saturated by a nanofluid, Int. J. Heat Mass Transfer, 52, 5792–5795, (2009).

[26] A.V. Kuznetsov, D.A. Nield, Natural convective boundary- layer flow of a nanofluid past a vertical plate, Int. J. Therm. Sci., 49, 243–247, (2010).

[27] M. Turkyilmazoglu, I. Pop, Heat and mass transfer of unsteady natural convection flow of some nanofluids past a vertical infinite flat plate with radiation effect, Int. J. Heat Mass Transfer 59, 167–171, (2013).

[28] A.V. Kuznetsov, D.A. Nield, Natural convective boundary-layer flow of a nanofluid past a vertical plate: A revised model, Int. J. of Therm. Sci. 77, 126-129, (2014).

[29] M. Sheikholeslami, D.D. Ganji, M.Y. Javedb, R. Ellahi, Effect of thermal radiation on magnetohydrodynamics nanofluid flow and heat transfer by means of two phase model, J. Magn. Magn. Mat., 374, 36–43, (2015).

[30] H. Zargartalebi, A. Noghrehabadi,·M. Ghalambaz, I. Pop, Natural convection boundary layer flow over a horizontal plate embedded in a porous medium saturated with a nanofluid: case of variable thermophysical properties, Transp Porous Med., 107, 153–170, (2015)

[31] M.B. Ben Hamida, K. Charrada, Natural convection heat transfer in an enclosure filled with an ethylene glycol—copper nanofluid under magnetic fields, Numer. Heat Transfer, Part A, 67, 902–920, (2015).

[32] S. Agarwal, M. Kumar, C. Shakher, Temperature measurement of axisymmetric flames under the influence of magnetic field using Talbot interferometry, AIP Conf Proc, 1620, 485–491, (2014).

[33] M.J. Uddin, O.A. Bég, N. Amin, Hydromagnetic transport phenomena from A stretching or shrinking nonlinear nanomaterial sheet with Navier slip and convective heating: A model for bio-nano-materials processing, J. of Mag. and Mag. Mat., 38,252–261, (2014).

[34] R. Azizian, E. Doroodchi, T. McKrell, J. Buongiorno, L. W. Hu, B. Moghtaderi, Effect of magnetic field on laminar convective heat transfer of magnetite nanofluids, Int. J. of Heat and Mass Transfer, 68,94-109, (2014).

[35] B. Mehdi, M. Hangi, Flow and heat transfer characteristics of magnetic nanofluids: A review, J. of Mag. and Mag. Mat., 374,125–138(2014)

[36] A.E. Kabeel, Emad M.S. El-Said, S.A. Dafea, A review of magnetic field effects on flow and heat transfer in liquids: Present status and future potential for studies and applications, Renew. and Sus. Ener. Rev., 45, 830–837, (2015).

[37] M.A.A. Hamad, Analytical solution of natural convection flow of a nanofluid over a linearly stretching sheet in the presence of magnetic field, Int. Commun. Heat Mass Transf., 38, 487–492, (2011).

[38] M. Govindaraju, N. Vishnu Ganesh, B. Ganga, A.K. Abdul Hakeem, Entropy generation analysis of magneto hydrodynamic flow of a nanofluid over a stretching sheet, J. Egypt. Math. Soc., (2015). doi.org/10.1016/j.joems.2014.04.005.

[39] N.V. Ganesh, A.K.A. Hakeem, R. Jayaprakash, B. Ganga, Analytical and numerical studies on hydromagnetic flow of water based metal nanofuids over a stretching sheet with thermal radiation effect, J. Nanofluids, 3,154–161, (2014).

[40] M.M. Rashidi, N. Vishnu Ganesh, A.K. Abdul Hakeem, B. Ganga, Buoyancy effect on MHD flow of nanofluid over a stretching sheet in the presence of thermal radiation, J. Mol. Liq., 198, 234–238, (2014).

[41] GH.R. Kefayati, Magnetic field effect on heat and mass transfer of mixed convection of shear-thinning fluids in a lid-driven enclosure with non-uniform boundary condition, J. of the Taiwan Ins. of Chem. Eng., In Press.

[42] A.K.A. Hakeem, N. Vishnu Ganesh, B. Gang, Magnetic field effect on second order slip flow of nanofluid over a stretching/shrinking sheet with thermal radiation effect, J. of Mag. and Mag. Mat., 381, 243-257, (2015).

[43] R. Dhanai, P. Rana, K. Lokendra, Lie group analysis for bioconvection MHD slip flow and heat transfer of nanofluid over an inclined sheet: Multiple solutions, J. of the Taiwan Ins. of Chem. Eng. 66, 283-291(2016).

[44] R. Dhanai, P, Rana, K. Lokendra, Multiple solutions in MHD flow and heat transfer of Sisko fluid containing nanoparticles migration with a convective boundary condition: Critical points, The Euro. Phy. J. Plus 131, 1-14 (2016).

[45] R. Dhanai, P Rana, K. Lokendra, Critical values in slip flow and heat transfer analysis of non-Newtonian nanofluid utilizing heat source/sink and variable magnetic field: Multiple solutions, J. of the Taiwan Ins. of Chem. Eng. 58, 155-164(2016).

[46] M.J. Uddin, P Rana, O. A. Bég, A.I.M. Ismail, Finite element simulation of magnetohydrodynamic convective nanofluid slip flow in porous media with nonlinear radiation, Alexan. Eng. J. (2016).

[47] P. Rana, M. J. Uddin, Y. Gupta, A. I. M. Ismail, Two-component modeling for non-Newtonian nanofluid slip flow and heat transfer over sheet: Lie group approach, Appl. Math. and Mecha. 37, no. 10, 1325-1340 (2016).

[48] P. Rana, R. Dhanai, K Lokendra, Radiative nanofluid flow and heat transfer over a non-linear permeable sheet with slip conditions and variable magnetic field: Dual solutions, Ain Shams Eng. J. (2015).

[49] K. Pradhan, S. Samanta, A. Guha, Natural convective boundary layer flow of nanofluids above an isothermal horizontal plate, ASME J. of Heat Transfer, 136,102501, (2014).

[50] G. Karniadakis, A. Beskok and N. Aluru, In: Microflows and Nanoflows Fundamentals and Simulation. Springer Science, New York, 2005.

[51] I. Vleggaar, Laminar boundary layer behaviour on continuous, accelerating surfaces. Chem Eng Sci 32,1517-25,(1977).

[52] F.A. Fathalah, A.M. Elsayed, Natural convection due to solar radiation over a non-absorbing plate with and without heat losses, Int. J. Heat Fluid Flow, 2, 41-45, (1980).

[53] R. Cortell, MHD (magneto-hydrodynamic) flow and radiative nonlinear heat transfer of a viscoelastic fluid over a stretching sheet with heat generation/absorption, Energy 74, 896-905, (2014).

[54] E.M. Sparrow, R.D. Cess, Radiation Heat Transfer. Hemisphere, Washington (Chaps. 7 & 10) 1978.

[55] P.K.H Ma, W.H. Hui, Similarity solutions of the two-dimensional unsteady boundary-layer equations, J. of Fluid Mech., 216, 537-559, (1990).

[56] D. Kolomenskiy, H.K. Mofatt, Similarity solutions for unsteady stagnation point flow, J. Fluid Mech., 711, 394-41, (2012).

[57] S. Asghar, M. Jalil, M. Hussan, M. Turkyilmazoglu, Lie group analysis of flow and heat transfer over a stretching rotating disk, Int. J. of Heat and Mass Transfer 69, 140–146, (2014)

[58] J. Uddin, O.A. Bég, A. Aziz, A.I.Md Ismail, Group analysis of free convection flow of a magnetic nanofluid with chemical reaction, Math Prob in Eng., 2015 (2015), Article ID 621503, 11 pages. doi.org/10.1155/2015/621503.

[59] R. Seshadri, T.Y. Na, Group Invariance in Engineering Boundary Value Problems, Springer, New York, 1985.

[60] P.J. Olver, Application of Lie Groups to Differential Equations, Springer, NewYork, NY, USA, 1989.

[61] B.J. Cantwell, Introduction to Symmetry Analysis, Cambridge University Press, 2003.

[62] G.W. Bluman, S.C. Anco, Symmetry and Integration Methods for Differential Equations, Springer, New York, 2009.

[63] S. Siddiqa, MA.A. Hossain, S.C. Saha, The effect of thermal radiation on the natural convection boundary layer flow over a wavy horizontal surface. Int. J. of Therm. Sci., 84, 143-150, (2015).

[64] A. Pantokratoras, T. Fang, Sakiadis flow with nonlinear Rosseland thermal radiation, Phys. Scr., 87 015703 (5pp), (2013).

[65] M. Imtiaz, T. Hayat, M. Hussain, S.A. Shehzad, G.Q.B. Ahmad, Mixed convection flow of nanofluid with Newtonian heating, The Euro. Phy. J. Plus, 129, 1-11, (2014).